PAPER

Check for updates

Fluorescent probe for Cu²⁺ and the secondary application of the resultant complex to detect cysteine†

Meipan Yang, [ID] *[abc] Lifeng Ma,[abc] Jing Li[abc] and Longli Kang*[abc]

A special fluorescent probe has been developed, one that demonstrated excellent "off-on-type" change in fluorescence with high selectivity toward Cu²⁺. Interestingly, the probe–Cu²⁺ complex could detect cysteine due to the ability of this amino acid to strongly coordinate Cu²⁺, and no obvious interference was observed from other amino acids and anions. According to the proposed mechanism, addition of cysteine induced decomplexation of the probe–Cu²⁺ form. Furthermore, the results of confocal microscopy experiments demonstrated the potential of using the probe to image Cu²⁺ in living cells and mice.

Introduction

As the third most abundant transition metal ion, copper is an essential element for life and plays vital roles in various biological processes. Its homeostasis is critical for the metabolism and development of living organisms.[1–3] Fluorescent probes have been developed to meet the demand for molecular recognition tools. Fluorescent probes combine molecular recognition with fluorometric analysis and have as a result expanded applications. When reacting with or binding to an acceptor in a specific manner, the fluorophore of the probe could express the recognition process in the form of an optical signal. In recent years, several fluorescent probes for Cu²⁺ have been reported, and some of them have been successfully applied both in biological and environmental samples.[4,5] Rhodamine derivatives bearing a spirolactam structure are non-fluorescent (off), whereas ring opening of the corresponding spirolactam gives rise to a strong fluorescence emission (on). So the study of outstanding probes for Cu²⁺ based on rhodamine is ongoing.

Cysteine (Cys) is an important amino acid and biothiol, and plays an essential role in many significant cellular functions such as protein synthesis, detoxification, and metabolism.[6,7] A deficiency of cysteine may lead to many syndromes such as slow growth in children, hair depigmentation, lethargy and liver damage.[8–10] On the other hand, elevated levels of cysteine have

been associated with cardiovascular disease, Alzheimer's disease, neural tube defects, and osteoporosis.[11–13] Li and co-workers[14] developed a novel ratiometric Cys-selective fluorescence probe. The biocompatible merocyanine probe showed highly selective detection and monitoring of Cys. The probe has been successfully applied to the ratiometric imaging and detection of mitochondrial Cys in cells and intact tissues. From the biological and pharmacological points of view, the detection of cysteine is particularly critical for the early diagnosis and treatment of related diseases.

Nowadays, fluorescence-based detection methods have been widely applied in the detection of biologically relevant ions and bio-molecules due to their advantages of being simple and highly sensitive. In the past few years, various fluorescent probes that detect thiols have been developed based on different mechanisms such as Michael addition,[15–18] cyclization reaction with aldehyde,[19–21] cleavage reaction induced by thiols,[22–25] nucleophilic aromatic addition,[26,27] and ligand displacement of metal complexes by thiols.[28–30] Most of these fluorescent-labeling reagents contain a functional group, e.g., N-substituted maleimide, reactive halide or aziridine, that reacts with thiol groups in general, and thus are not specific to Cys.[31,32] The common way developed to detect Cys is the so-called "chemosensing ensemble". In this method, the fluorescent indicator is bound to the receptor through non-covalent interactions (such as coordination), and the fluorescence of the indicator is either quenched or enhanced by the receptor.[33–35] The precise interactions between cysteine and copper in biological systems remain unknown. Of the 20 predominant biological amino acids, cysteine has a particularly strong binding affinity towards copper.[36] Cu²⁺ could be recognized by the designed probe, and then Cys may be detected secondly by using the probe–Cu²⁺ complex. Qian and co-workers[37] have synthesized a new rhodamine-based fluorescent chemosensor that can selectively and sensitively recognize Cu²⁺ and Zn²⁺ in

Key Laboratory for Molecular Genetic Mechanisms and Intervention Research on High Altitude Disease of Tibet Autonomous Region, School of Medicine, Xizang Minzu University, Xianyang, 712082, China. E-mail: ymp1111@126.com; klongli@163.com

Key Laboratory of High Altitude Environment and Gene Related to Disease of Tibet Autonomous Region, School of Medicine, Xizang Minzu University, Xianyang, 712082, China

Key Laboratory for Basic Life Science Research of Tibet Autonomous Region, School of Medicine, Xizang Minzu University, Xianyang, 712082, China

† Electronic supplementary information (ESI) available. See DOI: 10.1039/c9ra02360g

different solutions. In addition, the zinc-containing complex shows selective recognition for His/Cys. Zhang and co-workers[38] synthesized a probe for the specific detection of cysteine and homocysteine in water. The detection can be performed by observing the color changes from yellow to red upon addition of cysteine or homocysteine without interference by other amino acids. Wang and co-workers[39] demonstrated the use of a molecular probe for the sensitive detection of cysteine in human plasma. The sensing mechanism was shown to involve release of the fluorescent probe from a non-fluorescent probe–copper complex upon exposure of the complex to Cys. The new dye was shown to have the desired properties suitable for bio-sensing applications. The ultimate goals of our research are designing and synthesizing "one-to-two" or even "one-to-many" probes for which high efficiency is achieved by a simultaneous functioning of probes operating based on different mechanisms. Sensitive identification of two or more target materials to maximize the use of resources has vitally important application values.

Keeping these goals in mind, we produced a probe for Cu^{2+}, and then explored the ability of the probe–Cu^{2+} complex to detect Cys. The probe showed excellent recognition of Cu^{2+}, with obvious absorption and fluorescence. Upon addition of Cys to the probe–Cu^{2+} complex solution, Cys was detected apparently by capturing Cu^{2+} from the probe–Cu^{2+} complex. Then the probe recovered the structure of the rhodamine lactam ring, and the absorption and fluorescence disappeared.

Experimental

Synthesis

The synthetic route to the target probe is shown in Scheme 1. Compound **1** was obtained according to the literature.[40]

Rhodamine B hydrazide was synthesized following the reported procedure.[41,42] Rhodamine B hydrochloride (2.4 g, 0.005

mol) was dissolved in 20 mL of ethanol. Then, to this solution, an excess amount of hydrazine hydrate (3 mL) was added dropwise and the resulting reaction mixture was refluxed for 2 h. The mixture was then cooled, poured into water, and extracted with ethyl acetate. Finally, the solution was dried with anhydrous sodium sulfate, filtered, and then gave rhodamine B hydrazide.

Rhodamine B hydrazide (4.56 g, 10 mmol) was dissolved in 20 mL of ethanol, to which compound **1** (15 mmol) was then added, followed by stirring of the resulting the mixture for 6 h at room temperature. After that, the solvents were dried *in vacuo* and the crude product was purified by performing chromatography on silica gel. Yellow solid, yield: 53%. ^{1}H NMR (400 MHz, CDCl$_3$) δ (ppm) 11.44 (s, 1H), 9.12 (s, 1H), 8.05–7.90 (m, 1H), 7.83 (d, J = 12.0 Hz, 2H), 7.79 (d, J = 8.0 Hz, 1H), 7.69 (s, 1H), 7.60–7.46 (m, 2H), 7.18 (d, J = 8.0 Hz, 1H), 7.05–6.90 (m, 3H), 6.60–6.40 (m, 4H), 6.32–6.22 (m, 2H), 3.88 (s, 3H), 3.33 (q, J = 8.0 Hz, 8H), 1.16 (t, J = 6.5 Hz, 12H). ^{13}C NMR (100 MHz, CDCl$_3$) δ 163.5, 161.7, 154.9, 152.5, 149.9, 149.7, 148.1, 147.2, 144.5, 132.8, 128.3, 127.7, 127.5, 127.0, 124.8, 124.5, 123.7, 123.2, 122.5, 122.1, 117.8, 117.2, 115.1, 107.1, 103.9, 96.9, 65.5, 43.3, 11.6. HRMS (ESI) calcd. for $C_{42}H_{42}N_6O_4$ [M + H]$^+$: 695.3340, found: 695.3343.

Materials and instrumentation

The fluorescence spectra and relative fluorescence intensity were obtained with a HITACHI F-4500 fluorescence spectrophotometer. The absorption spectra were acquired using a Shimadzu UV-1700 spectrophotometer at room temperature. Mass spectra (ESI-MS) were collected using an AXIMA-CFRTM plus MALDI-TOF mass spectrometer. ^{1}H and ^{13}C NMR spectra were recorded on a Varian INOVA-400 MHz spectrometer with tetramethylsilane (TMS) as an internal standard. Imaging of live mice was conducted employing an Xenogen IVIS spectrum imaging system. Chromatographic separations were done using Merck silica gel (250–400 mesh ASTM). Thin-layer chromatography (TLC) was performed on silica gel GF254.

Double distilled water was used throughout the experiment. Unless specifically noted, the solvents and reagents were purchased from commercial sources and used as received. Rhodamine B, *p*-anisidine and salicylaldehyde were purchased from Aladdin (http://www.aladdin-e.com/zh_cn/). Hydrazine hydrate was purchased from Sinopharm Chemical Reagent Co., Ltd (https://www.reagent.com.cn/).

General procedures used to collect spectra for detection

Solutions of probe and detected ions (or amino acids) were prepared in methanol–water (3/7, v/v). The ions and amino acids tested were Fe^{3+}, NH_4^+, Ag^+, Ba^{2+}, Al^{3+}, Cd^{2+}, Cr^{3+}, Sn^{2+}, Hg^{2+}, Mg^{2+}, Mn^{2+}, Na^+, Ni^{2+}, Pb^{2+}, Zn^{2+}, Cl^-, Br^-, SO_4^{2-}, SCN^-, S^{2-}, $C_2O_4^{2-}$, NO_3^-, NO_2^-, CN^-, Hcy, GSH, Gly, Glu, Ala, Pro, His and Ser. Fresh solutions used for spectroscopic measurements were made by diluting stock solutions. Each sample was shaken for 10 s and then allowed to sit for 20 min at room temperature before taking the measurement. The excitation wavelength was
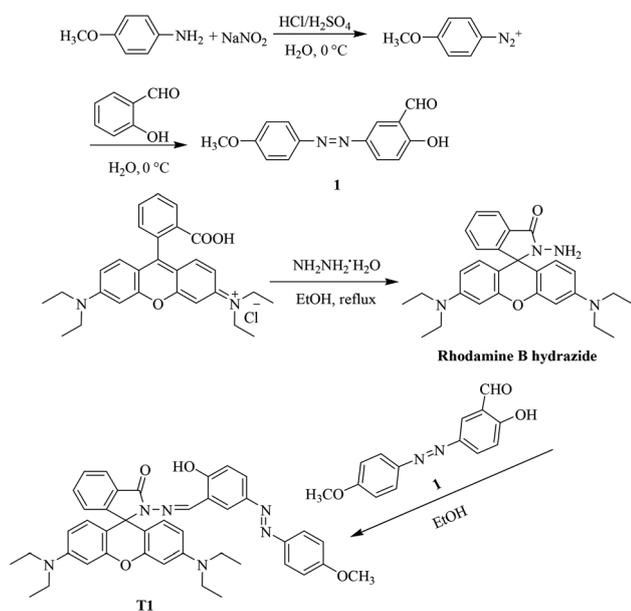
Scheme 1 Synthesis of the probe.

535 nm. The bandpass was set to 2.5 nm for this excitation wavelength and 5.0 nm for the emission wavelength.

Fluorescence imaging for cells and mice

The HepG2 cells were cultured in Roswell Park Memorial Institute (RPMI) 1640 supplemented with 10% fetal bovine serum (FBS). Immediately before performing the experiments, cells were pretreated with probe (20 μM) for 1 h at 37 °C in humidified air and 5% CO_2, washed three times with phosphate-buffered saline (PBS) and imaged. After incubation with $CuCl_2$ (40 μM) for another 2 h, the cells were washed 3 times with PBS and imaged.

All animal procedures for this study were followed in accordance with the requirements of the National Act on the use of experimental animals (China) and were approved by the Ethnics Committee of the medical department of Xizang Minzu University. The Kunming mouse (20–25 g) was given an intra-peritoneal (i.p.) injection of probe (400 μL × 400 μM). The mouse was anesthetized by being made to inhale isoflurane and then imaged by using an imaging system. Then, $CuCl_2$ (40 μL × 40 μM) was injected into the same region; and after 10 min, the mouse was then imaged again.

Results and discussion

Structural properties

The procedures used to synthesize probe **T1** are summarized in the Scheme 1, and the structure was determined using various spectroscopic techniques, in particular ^1H NMR, ^{13}C NMR and mass spectroscopies.

Spectral characteristics of the probe for Cu^{2+}

As shown in Fig. 1, free probe **T1** showed neither any absorption nor fluorescence, which was ascribed to the free probe adopting predominantly the spirolactam form. When Cu^{2+} was added to the probe solution (10 μM), a notable enhancement of absorption appeared at a wavelength of 552 nm. As the concentration

of Cu^{2+} was increased, the absorption intensity also increased. These results indicated that the addition of Cu^{2+} induced the opening of the five-membered spiral ring of rhodamine. Further, the fluorescence spectra of the probe and Cu^{2+} were investigated. With the addition of Cu^{2+}, a new emission peak appeared at 588 nm, which was attributed to the opening of the lactam ring in rhodamine. For concentrations of Cu^{2+} between 0 and 10 μM, the relationship between fluorescence intensity and concentration was found to be quite linear (Fig. S1†).

Selectivity is an important criterion for measuring probe performance. Fig. 2 shows the selectivity of 10 μM **T1** after 10 μM of various common cations (including Fe^{3+}, NH_4^+, Ag^+, Ba^{2+}, Al^{3+}, Cd^{2+}, Cr^{3+}, Sn^{2+}, Hg^{2+}, Mg^{2+}, Mn^{2+}, Na^+, Ni^{2+}, Pb^{2+}, and Zn^{2+}) were each added to a separate probe solution sample. Only the addition of Cu^{2+} generated a new absorption peak at 552 nm. The fluorescence spectrum also showed similar changes.

The tolerance of the probe (10 μM) during its detection of Cu^{2+} (10 μM) is displayed in Fig. 3. As expected, the Cu^{2+}-induced spectral enhancement was not affected by the presence of any other tested background metal ion (20 μM) in a meth-anol–water (3/7, v/v) solution. These results showed the strong anti-interference ability of the probe.

Spectral characteristics of the probe for Cys in the presence of Cu^{2+}

Kinetic studies. As the optical signal in our experiments relied on the chemical reaction between the probe–Cu^{2+} complex and Cys, the reaction rate might have affected the experimental results. Thus, kinetics studies using the detecting system were undertaken and the results are shown in Fig. S2.† The results showed that the fluorescence response decreased quickly after addition of Cys, and the recognition interaction completed within 4 min, indicating the potential effectiveness of using the probe–Cu^{2+} complex for the real-time monitoring of Cys. Meanwhile, based on these results, a reaction time of 4 min was used in subsequent experiments with the system.
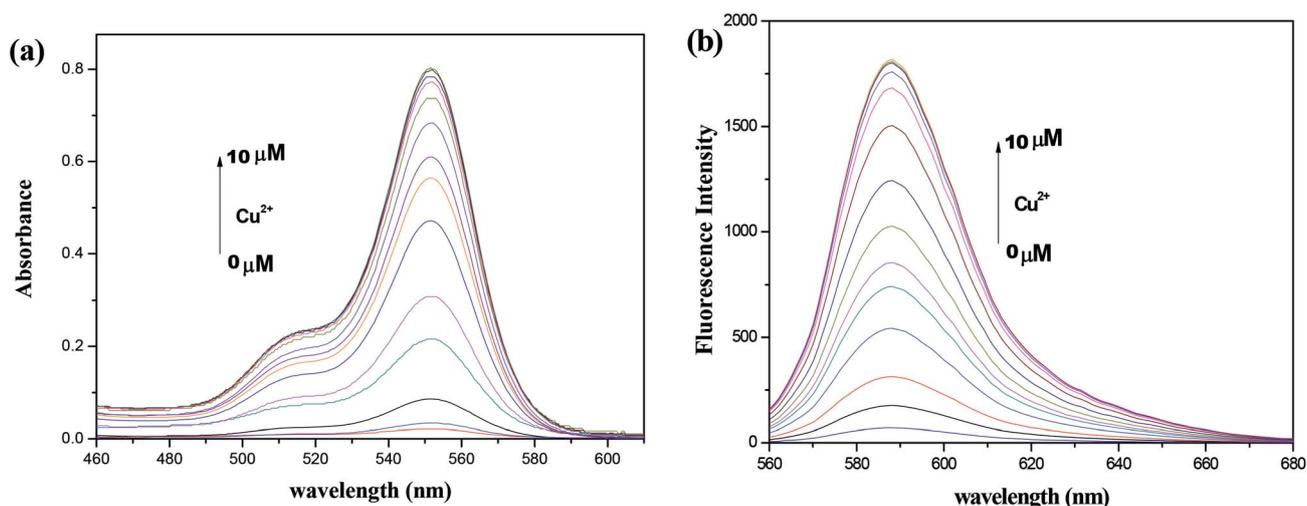

Fig. 1 Absorption spectra (a) and fluorescence spectra (b) of the synthesized probe (10 μM) with various amounts of Cu^{2+}. λ_{ex} = 535 nm.
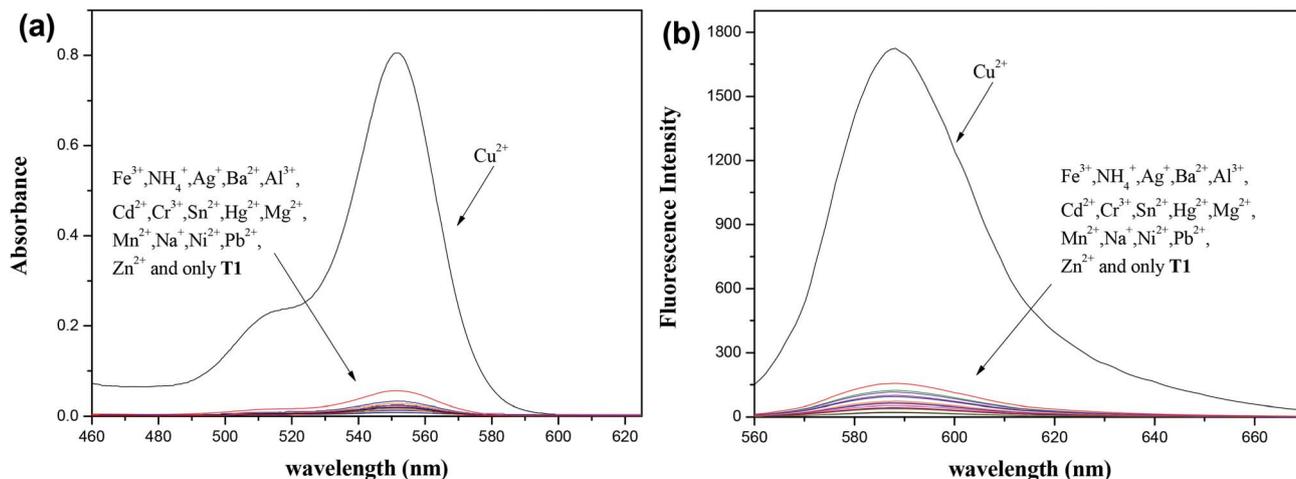
Fig. 2 UV-Vis absorption spectra (a) and fluorescence spectra (b) of the probe (10 μM) with various ions (10 μM), with each experiment carried out in a methanol–water (3/7, v/v) solution. $\lambda_{ex} = 535$ nm.

UV-Vis absorbance and fluorescence spectra of probe–Cu^{2+} titrated with Cys. Previously, according to the strategy involving the displacement of Cu^{2+}-chelating ligands, Cys can be detected based on its ability to strongly coordinate Cu^{2+}. Thus, we hypothesized that the probe–Cu^{2+} complex would be an effective fluorescent probe for Cys. To test this hypothesis, we compared UV-Vis absorbance and fluorescence spectra of the probe–Cu^{2+} complex collected before and after adding Cys. Based on our previous study, the solution of the probe–Cu^{2+} complex (10 μM probe and 10 μM Cu^{2+}) demonstrated an obvious absorption at the wavelength of 552 nm. With the addition of Cys (0–20 μM) to the above solution, the absorption intensity gradually decreased, which was due to the disappearance of the conjugated system, and the wavelength blue shifted (Fig. 4a). This phenomenon indicated that Cys could capture Cu^{2+} from the probe–Cu^{2+} complex, and the probe adopted the spirocycle form with neither significant UV-Vis absorption nor fluorescence. A similar phenomenon was also observed in the fluorescence changes (Fig. 4b). As depicted in Fig. S3,† the detection limit of Cys was approximately 1.2×10^{-6} M based on the literature definition of the detection limit.[43] In a word, the decrease of the UV-Vis absorbance and fluorescence of probe–Cu^{2+} by the addition of Cys both indicated that Cys pulled Cu^{2+} from the complex, and that the spirocycle form of probe was recovered via interaction of Cys with probe–Cu^{2+}.

Selectivity and tolerance of the probe–Cu^{2+} system to Cys. Metal ionic complexes are considered to be ideal for use in approaches aimed at recognizing anions and amino acids. Thus, the selectivity of the probe–Cu^{2+} complex for 20 μM of relevant anions and amino acids (including Cl^-, Br^-, SO_4^{2-}, SCN^-, S^{2-}, $C_2O_4^{2-}$, NO_3^-, NO_2^-, CN^-, Hcy, GSH, Gly, Glu, Ala, Pro, His and Ser) was determined. As shown in Fig. 5, both the intensity of the absorption and emission were decreased only with the addition of Cys, whereas the tested anions and other amino acids produced poor changes in the spectra. The stronger binding of Cys with Cu^{2+} than with the probe clearly contributed to the high sensitivity in the detection of Cys and was also responsible for the good selectivity over other examined substances.

In addition, whether the **T1**–Cu^{2+} complex (10 μM probe and 10 μM Cu^{2+}) could still retain the sensing response to Cys under the potential interferent was considered to be very important for the applicability of this fluorescent probe. As shown in Fig. S4,† the addition of Cys still resulted in large fluorescence changes even in the presence of 2.0 equiv. of interferents. The competitive anions tested showed virtually no influence on the fluorescence detection of Cys. These observations indicated that the probe–Cu^{2+} complex could serve as a potentially effective probe of Cys with excellent properties.
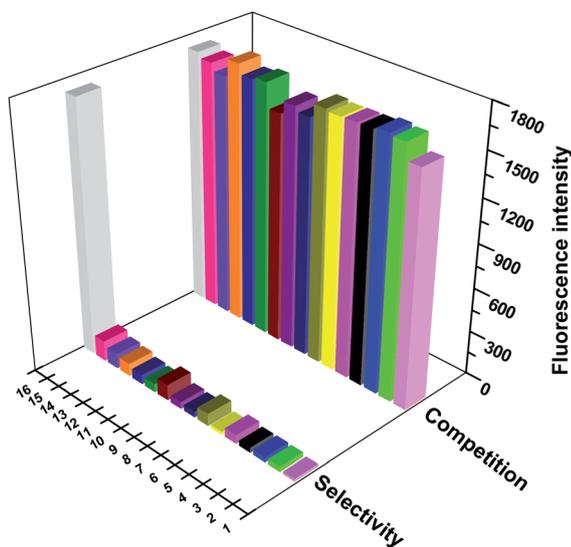

Fig. 3 The selectivity and competition of the probe for Cu^{2+}. The pillars in the front row represent the respective fluorescence responses of the probe (10 μM) for the examined metal ions. The pillars in the back row each represent the response after subsequent addition of 10 μM Cu^{2+} to the solution containing the probe and the competing metal ion (20 μM), namely Fe^{3+}, NH_4^+, Ag^+, Ba^{2+}, Al^{3+}, Cd^{2+}, Cr^{3+}, Sn^{2+}, Hg^{2+}, Mg^{2+}, Mn^{2+}, Na^+, Ni^{2+}, Pb^{2+}, Zn^{2+}, or Cu^{2+} from 1 to 16.
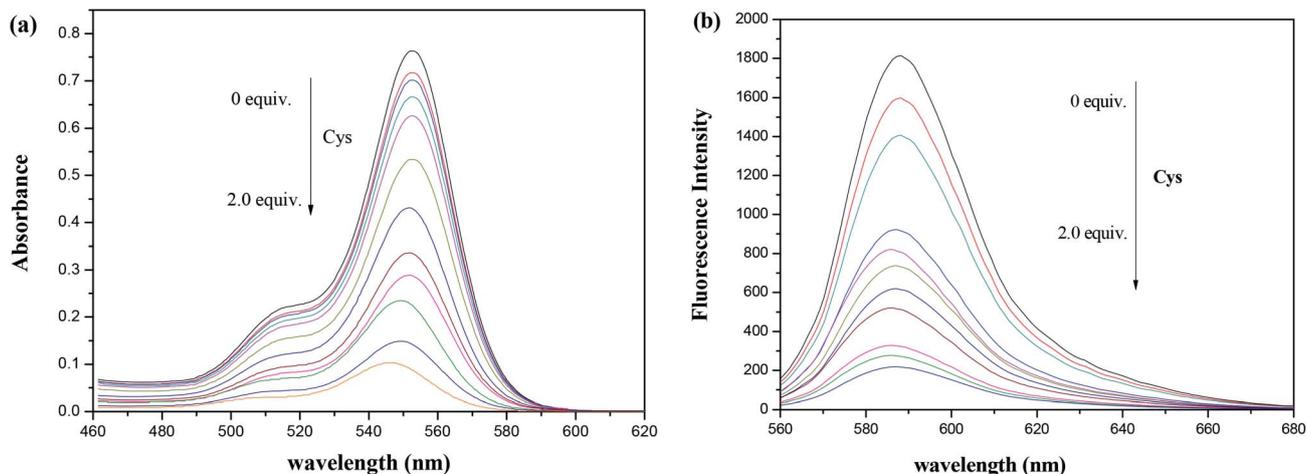
Fig. 4 Absorption spectra (a) and fluorescence spectra (b) of the probe–Cu^{2+} complex with various amounts of Cys. λ_{ex} = 535 nm.
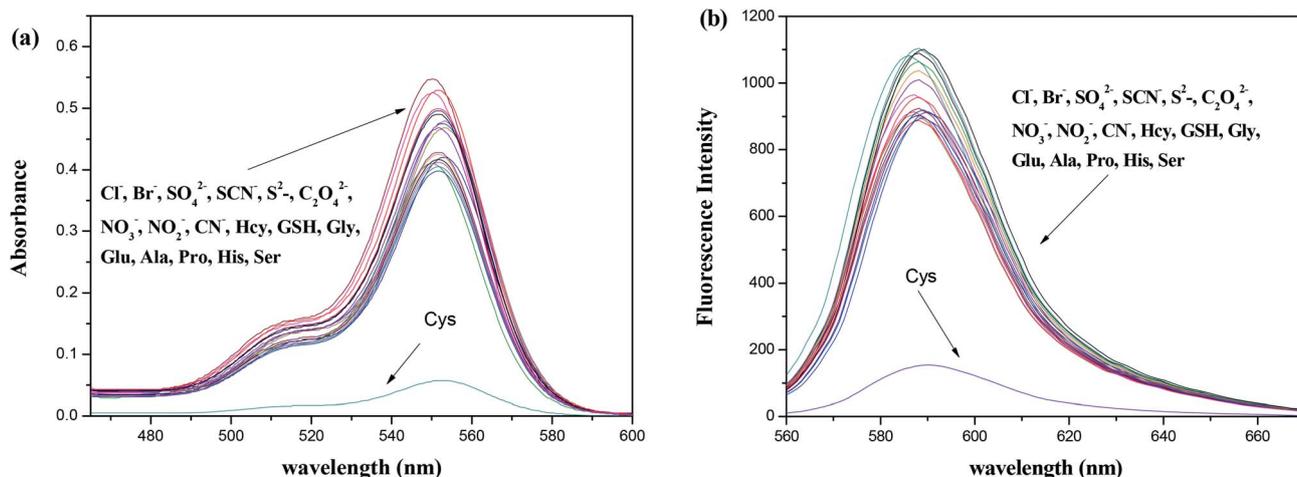

Fig. 5 UV-Vis absorption spectra (a) and fluorescence spectra (b) of the probe–Cu^{2+} complex upon addition of various anions or amino acids (20 μM), with each experiment carried out in a methanol–water (3/7, v/v) solution. λ_{ex} = 535 nm.
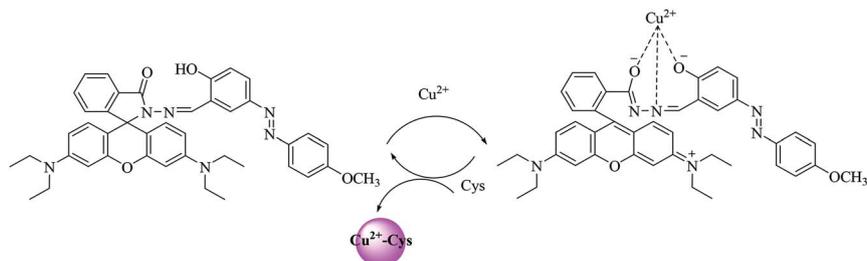
Mechanism

DFT calculations based on the Fukui function $f_+(r)$ were further carried out for **T1** by using the Gaussian 09 program to explore the binding site better. The double-ζ quality (6-31 + G* for O and N, 6-31G** for C and H) basis set was applied for the geometry optimization and the following single-point energy calculation. According to the results of the vibration analysis, the optimized structure was proven to be the local minimum. Based on NBO analysis,[44] the condensed Fukui functions of carbonyl O (0.026) and hydroxyl O (0.028) were larger than those of N1 (−0.001) and N2 (−0.002). These results indicated that the probe was most likely to chelate Cu^{2+} *via* carbonyl O and hydroxyl O (Fig. S5†).

From the mass spectrum (Fig. S6†), a unique peak at an *m/z* of 756.2475, corresponding to [**T1** + Cu–H]$^+$, was clearly observed, demonstrating the formation of the **T1**–Cu^{2+} complex. Interestingly, the intensity of the peak at an *m/z* of 695.3342 increased a bit after addition of Cys to the **T1**–Cu^{2+}

complex, corresponding to [**T1** + H]$^+$. This result indicated that the probe recovered the spirocyclic form under the present conditions.

Based on the various experiments that we carried out, a plausible mode of the binding of probe to Cu^{2+} and the progression to a secondary recognition of Cys was derived, and is shown in Scheme 2. Generally, the d orbital of Cu^{2+} is not underfilled by electrons, and the unpaired electrons lead to Cu^{2+} exhibiting paramagnetic properties, which make Cu^{2+} act as typical fluorescence quencher. In the meantime, the excellent photophysical properties of rhodamine, such as strong fluorescence emission and high fluorescence quantum yield, should be taken into consideration. Energy and electron transfer occurring when combining Cu^{2+} with the probe was expected to only cause partial loss of fluorophore emission energy. In general, the intensity of the fluorescence of the probe was observed to increase when Cu^{2+} bound. The flowing electrons of the Schiff base structure (–C=N–) of the probe was expected to cause a fluorescence emission. Azo dyes can be used

Scheme 2 Proposed mechanism used by the probe to recognize Cu^{2+} and Cys.
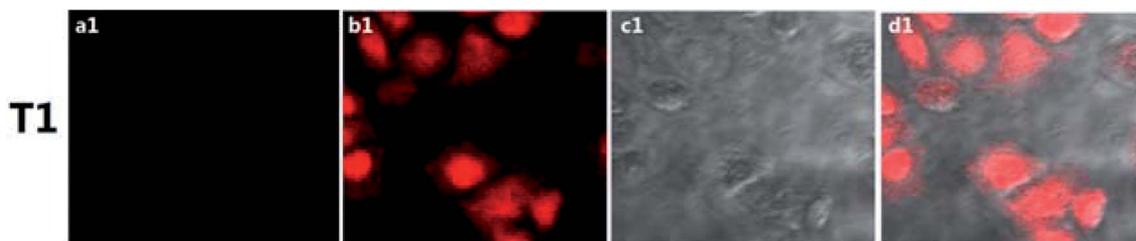

Fig. 6 Bioimaging applications of the probe in HepG2 cells. Representative fluorescence images of the cells treated with the probe (20 μM) in either the absence (a) or the presence (c) of 20 μM Cu^{2+} for 1.5 h at 37 °C. (b) Bright-field image of cells. (d) Overlay image of (b) and (c).

to further increase the extent of the molecular conjugation of a system, and hence was expected in our experiments to serve as an effective chromophore group for the detection of ions. The combination of the two frameworks was expected to yield a novel fluorescent reagent with excellent properties. At the same time, oxygen atoms are classified as hard bases according to the hard and soft acid and base principle. As a result, increasing the number of oxygen atoms was expected to increase the ability of the probe to complex with Cu^{2+}. In our experiments, these features indeed appeared to be beneficial for increasing the intensity of emission signals for yielding a better detection. Then, in the azophenol structure of the probe, the complexation of the Cu^{2+} with the phenolic hydroxyl group apparently effectively changed the distribution of charges in the molecule and realized the detection of Cu^{2+}.

In summary, the complexation of Cu^{2+} with the probe induced the opening of the rhodamine lactam ring, resulting in an obvious increase in absorption and fluorescence. Cys, when added to this solution, apparently captured Cu^{2+}, due to its ability to relatively strongly coordinate Cu^{2+}, and then led to the lactam ring of the probe having formed again and to the UV-Vis absorption and fluorescence signals having nearly disappeared.

Fluorescence imaging

For biological research applications, low toxicity is a prerequisite. The toxicity of the probe to HepG2 cells was explored by using the (3,4,5-dimethyl-2-thiazolyl)-2,5-diphenyl-2-*H*-tetrazolium bromide (MTT) assay method[45] with working concentrations of 80, 40, 20, 10, and 5 μM. As shown in Fig. S7,† the cell viability was about 86% when the probe concentration was 20 μM, indicative of low toxicity of the probe to cells and that the probe could be used in the fields of cell labeling, detection and staining.

To further demonstrate the practical biological application of the probes, confocal microscopy experiments were carried out in living HepG2 cells. As shown in Fig. 6, the probe showed almost no fluorescence in the cells (Fig. 6a). After the addition of Cu^{2+}, an obvious fluorescence was observed (Fig. 6b). Bright-field transmission images of cells treated with Cu^{2+} and the probe revealed that the cells were viable throughout the imaging experiments (Fig. 6c). The probe could bind to Cu^{2+} specifically in cells. After the introduction of Cu^{2+}, the lactam ring of the probe molecule opened, and the fluorescence appeared. The above results showed the ability of the probe to display excellent cytocompatibility and permeability, features important for the effective use of reagents designed to detect intracellular Cu^{2+}.

Encouraged by the results of the intracellular detection of Cu^{2+}, we considered whether the probe can be further applied to fluorescence imaging in live animals. To test this idea, Kunming mice (20–25 g) were selected as the subjects of study, and the results of our experiments with these mice are shown in Fig. S8.† When the probe was injected intraperitoneally into a mouse, no fluorescence was observed (Fig. S8a†). When the mouse was injected with Cu^{2+} at the same region, a large fluorescence signal was noted. The results suggested the ability of the probe to be highly biocompatible with small animals and that it could be widely used in biological research.

Conclusions

In summary, we have developed a special fluorescent probe, on that showed "off-on" response to Cu^{2+} based on a ring-opening mechanism. Moreover, the ensemble probe–Cu^{2+} complex was shown to be an excellent sensory system for detecting Cys, indicating the promise of the metal-based complex as a tool to

detect this amino acid. We further showed the ability of using the probe for bio-imaging not only in cells but also in live mice. We expect the synthesized probe to find additional interesting applications as sensing and labeling agents in biology and medicine.

Conflicts of interest

There are no conflicts to declare.

Acknowledgements

References

1 J. A. Cotruvo Jr, A. T. Aron, K. M. Ramostorres and C. J. Chang, *Chem. Soc. Rev.*, 2015, **44**, 4400.
2 S. G. Kaler, *Nat. Rev. Neurol.*, 2011, 7, 15.
3 C. Vulpe, B. Levinson, S. Whitney, S. Packman and J. Gitschier, *Nat. Genet.*, 1993, **3**, 7.
4 F. Chen, G. Liu and Y. Shi, *Talanta*, 2014, **124**, 139.
5 M. Yang, W. Meng and X. Liu, *RSC Adv.*, 2014, **4**, 22288.
6 C. E. Paulsen and K. S. Carroll, *Chem. Rev.*, 2013, **113**, 4633.
7 K. G. Reddie and K. S. Carroll, *Curr. Opin. Chem. Biol.*, 2008, **12**, 746.
8 N. F. Ibrahim, *J. Radiat. Res. Appl. Sci.*, 2012, **5**, 647.
9 S. M. Marino and V. N. Gladyshev, *J. Mol. Biol.*, 2010, **404**, 902.
10 E. Weerapana, C. Wang, G. M. Simon, F. Richter, S. Khare, M. B. D. Dillon, D. A. Bachovchin, K. Mowen, D. Baker and B. F. Cravatt, *Nature*, 2010, **68**, 790.
11 C. Yee, W. Yang and S. Hekimi, *Cell*, 2014, **157**, 897.
12 S. Seshadri, A. Beiser, J. Selhub, P. F. Jacques, I. H. Rosenberg, R. B. D'Agostino, P. W. Wilson, P. A. Wolf and N. Engl, *J. Med.*, 2002, **346**, 476.
13 X. F. Wang and M. S. Cynader, *J. Neurosci.*, 2001, **21**, 3322.
14 W. Niu, L. Guo, Y. Li, *et al.*, *Anal. Chem.*, 2016, **88**, 1908.
15 Y. Q. Sun, M. Chen, J. Liu, X. Lv, J. F. Li and W. Guo, *Chem. Commun.*, 2011, **47**, 11029.
16 L. Wang, Q. Zhou, B. Zhu, L. Yan, Z. Ma, B. Du and X. Zhang, *Dyes Pigm.*, 2012, **95**, 275.
17 Z. Guo, S. Nam, S. Park and J. Yoon, *Chem. Sci.*, 2012, **3**, 2760.
18 D. Kand, A. M. Kalle, S. J. Varma and P. Talukdar, *Chem. Commun.*, 2012, **48**, 2722.
19 X. Liu, X. Na and S. Liu, *J. Mater. Chem.*, 2012, **22**, 7894.
20 H. Li, J. Fan and J. Wang, *Chem. Commun.*, 2009, 5904.
21 P. Wang, J. Liu and X. Lv, *Org. Lett.*, 2012, **14**, 520.
22 J. Shao, H. Sun and H. Guo, *Chem. Sci.*, 2012, **3**, 1049.
23 B. Tang, Y. Xing, P. Li, N. Zhang, F. Yu and G. Yang, *J. Am. Chem. Soc.*, 2007, **129**, 11666.
24 H. Y. Shiu, M. K. Wong and C. M. Che, *Chem. Commun.*, 2011, **47**, 4367.
25 Y. Chen, J. Zhao and H. Guo, *J. Org. Chem.*, 2012, **77**, 2192.
26 X. Chen, Y. Zhou, X. Peng and J. Yoon, *Chem. Soc. Rev.*, 2010, **39**, 2120.
27 X. Chen, S. K. Ko and M. J. Kim, *Chem. Commun.*, 2010, **46**, 2751.
28 L. Zhou, Y. Lin and Z. Huang, *Chem. Commun.*, 2012, **48**, 1147.
29 H. S. Jung, J. H. Han and Y. Habata, *Chem. Commun.*, 2011, **47**, 5142.
30 C. Luo, Q. Zhou, B. Zhang, *et al.*, *New J. Chem.*, 2011, **35**, 45.
31 W. Hao, A. Mcbride, S. Mcbride, *et al.*, *J. Mater. Chem.*, 2011, **21**, 1040.
32 G. Chwatko and E. Bald, *Talanta*, 2000, **52**, 509.
33 Y. Fu, H. Li, W. Hu, *et al.*, *Chem. Commun.*, 2005, 3189.
34 N. Shao, J. Y. Jin, S. M. Cheung, *et al.*, *Angew. Chem.*, 2010, **118**, 5066.
35 M. S. Han and D. H. Kim, *Tetrahedron*, 2004, **60**, 11251.
36 H. Lu, H. Zhang, J. Chen, *et al.*, *Talanta*, 2016, **46**, 477.
37 L. Xu, Y. Xu, W. Zhu, B. Zeng, C. Yang, B. Wu and X. Qian, *Org. Biomol. Chem.*, 2011, **24**, 8284.
38 D. Zhang, *Inorg. Chem. Commun.*, 2009, **12**, 1255.
39 W. Hao, A. McBride, S. McBride, J. P. Gao and Z. Y. Wang, *J. Mater. Chem.*, 2011, **21**, 1040.
40 J. Shao, *Dyes Pigm.*, 2010, **87**, 272.
41 Y. Xiang, A. Tong, P. Jin and Y. Ju, *Org. Lett.*, 2006, **8**, 2863.
42 M. Yang, W. Meng, X. Liu, N. Su, J. Zhou and B. Yang, *RSC Adv.*, 2014, **4**, 22288.
43 Z. Xu, L. Zhang, R. Guo, T. Xiang, C. Wu, Z. Zheng, *et al.*, *Sens. Actuators, B*, 2011, **156**, 546.
44 W. D. Chen, W. T. Gong, Z. Q. Ye, *et al.*, *Dalton Trans.*, 2013, **42**, 10093.
45 D. Horowitz and A. G. King, *J. Immunol. Methods*, 2000, **244**, 49.